Ceramics International 44 (2018) 3077–3084

Contents lists available at ScienceDirect

Ceramics International

journal homepage: www.elsevier.com/locate/ceramint

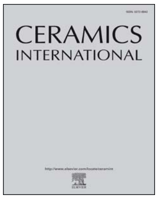

Graphenothermal reduction synthesis of MnO/RGO composite with excellent anodic behaviour in lithium ion batteries

P. Rosaiah[a,1], Jinghui Zhu[a,1], O.M. Hussain[b], Yejun Qiu[a,*]

[a] *Shenzhen Engineering Lab of Flexible Transparent Conductive Films, Department of Materials Science and Engineering, Shenzhen Graduate School, Harbin Institute of Technology, University Town, Shenzhen 518055, China*
[b] *Thin Film Laboratory, Department of Physics, Sri Venkateswara University, Tirupati 517502, Andhra Pradesh, India*

ARTICLE INFO

Keywords:
Reduced graphene oxide
MnO
Graphenothermal reduction
Anode
Li-ion batteries

ABSTRACT

Mn(II) oxide/graphene oxide (MnO/RGO) composites were synthesized by an easy and cost-effective graphenothermal reduction method. The surface morphology, structure, chemical composition and electrochemical behaviour of the resulting composites were investigated in detail. The MnO/RGO composite exhibited a high surface area (115.7 m^2/g), which led to the high discharge capacity, enhanced cycling stability, and outstanding rate capability as anode in Li-ion batteries (LIBs). The MnO/RGO composite exhibited an higher initial discharge capacity of 1607 mA h/g at a current density of 100 mA/g and maintained 94% of its reversible capacity over 100 consecutive cycles. Furthermore, MnO/RGO composite could preserve a significantly higher capacity of 847 mA h/g for 150 cycles even at a high current density of 250 mA/g. The excellent electrochemical properties result from the existence of highly conductive RGO and a short transportation span for both Li-ions and electrons. The developed MnO/RGO composite materials hold highly promising prospects in LIBs.

1. Introduction

Lithium ion batteries have drawn the extensive attentions as a potential candidate for the next generation energy-storage devices, owing to their desirable properties such as decent energy density, superior rate capability and extended cyclability [1–3]. The electrochemical performance of the electrode materials is the most vital factor to determine the whole property of LIBs [4,5]. Transition metal oxides (TMOs), such as manganese oxides, iron oxides, cobalt oxides and molybdenum oxides have attracted significant attention as electrode materials for LIBs because of their high theoretical capacities and environmental compatibility [6–9]. Among various TMOs, members of the manganese oxide family (MnO, MnO_2, Mn_2O_3, and Mn_3O_4) have paid significant attention as anode materials for LIBs owing to their excellent electrochemical properties [10–13]. Significantly, MnO takes advantage of its outstanding theoretical capacity (756 mAh/g), low operational potential and environmental affability has been recognized as a promising anode material for LIBs [14,15]. The conversion reaction between TMOs and lithium involves oxidation and reduction of metal nanoparticles, accompanied by an electrochemical process of the formation and decomposition of Li_2O, i.e. $MnO+2Li^{+}+2e^{-} \rightarrow Mn + Li_2O$ [16,17]. However, practical applications of pure MnO as an electrode material have limited not only by its poor capability and short cycle life arise from kinetic limitations but also larger volume change with charge-discharge processes [18,19].

Till now, tremendous effort with novel methodologies has been made to surmount the limitations of MnO based anode materials [20–22]. For example, some materials with a special morphology, including nanoparticles, nanorods, nanoplates, nanoflakes, nanotubes, nanoflower, were synthesized to facilitate the convenient migration of electrons and Li^{+} ions [23,24]. Moreover, the construction of nanocomposites with a carbon coating (which function as both conductive framework and volume buffer to improve the electrical conductivity and release internal stress), fabrication of hollow and/or porous nanostructures (these structures with high porosity can maintain higher capacity retention by reversibly tuning large volume changes), and embedding nanocomposite onto graphene (it has enhanced electronic conductivity, better cycle stability, and larger specific surface area) was also performed on promoting the electrochemical performance for LIBs [25,26]. Considering the complex fabrication procedures and novel methodologies, in this work, a simple and cost-effective hydrothermal and solid state graphenothermal reduction routes have been opting to prepare MnO_2 NWs and further to obtain MnO/RGO composites that can be directly used as a suitable anode material in LIBs.

---

[*] Corresponding author.
E-mail address: yejunqiu@hit.edu.cn (Y. Qiu).
[1] These authors contributed equally to this work.

https://doi.org/10.1016/j.ceramint.2017.11.070
Received 1 September 2017; Received in revised form 26 October 2017; Accepted 10 November 2017

2. Experimental section

2.1. Materials

Graphite flakes, manganese sulfate monohydrate ($MnSO_4{\cdot}H_2O$), concentrated sulfuric acid (H_2SO_4), potassium permanganate ($KMnO_4$), sodium nitrate ($NaNO_3$) and hydrogen peroxide (H_2O_2) were procured from Tianjin Yongda Chemical Reagent Corporation Limited. All these materials were directly employed without further treatment.

2.2. Preparation of graphene oxide (GO)

GO was prepared by a modified Hummer's process. In a typical synthesis of GO, 2 g of graphite flakes and 1 g of $NaNO_3$ were first placed in a 500 mL flask, followed by the dropwise addition of 50 mL of H_2SO_4 while stirring in an ice-bath. Subsequently, 6 g of $KMnO_4$ was slowly added to the reaction mixture. The system was continuously stirred until room temperature was reached. Afterward, the viscous mixture was diluted with 160 mL of pure-water, followed by the addition of 30% H_2O_2 to remove remnants of $KMnO_4$. The resultant mixture was centrifuged, washed with DI water and filtered. The final product (GO) was dried under vacuum at 70 °C for 24 h.

2.3. Preparation of MnO_2 NWs

MnO_2 NWs were synthesized by a hydrothermal synthesis route. In a typical synthesis, 1 mM aqueous solution of $KMnO_4$ was slowly dropped into 1 mM of $MnSO_4{\cdot}H_2O$ while continuously stirring. The aqueous H_2SO_4 solution was used to attune the pH (~ 2) of the mixture. After vigorous stirring for 10 h, the solution was reacted at 150 °C for 10 h with the application of Teflon-sealed stainless steel autoclave. After the reaction, the mixture was naturally cooled. The product was centrifuged, washed with DI water and ethanol. The final product was dried at 80 °C for 12 h.

2.4. Preparation of MnO/RGO

The obtained MnO_2 NWs were mixed with GO in 1:2 molar ratio and ground for half an hour using a mechanical grinder. The resultant reaction product was then placed in a ceramic boat and subsequently placed in a tube furnace. The temperature of the furnace was gradually increased to 650 °C at a rate of 5 °C/min with Argon (Ar) gas and maintained for 7 h. After the reaction, the mixture was naturally cooled under the continuous flow of Ar gas. The obtained black colour MnO/RGO composite powder was subsequently characterized directly without further treatments.

2.5. Material characterization

Surface morphological features were studied by FE-SEM (Model: HITACHI S-4700). TEM (Model: JEM 2010) was used to record morphology images and electron diffraction patterns of the samples. X-ray diffraction (XRD) (Model-Rigaku D/Max 2500/PC) patterns were recorded in the 2θ range 10–80 ° using CuKα radiation. Raman spectra were recorded in the wavenumber region from 100–2000 cm^{-1} using the Renishaw Raman system (Model-RM-1000) equipped with a Nd:YAG green laser as an excitation source. Thermogravimetric analysis (TGA) was performed in the temperature range from 30–1000 °C at a rate of 5 °C/min in N_2 ambiance. Specific surface area and porosity information of the samples were tested with the application of Brunauer-Emmett-Teller (BET) and Barrett-Joyner-Halenda (BJH) methods. The binding energy states of samples were characterized by X-ray photoelectron spectroscopy (XPS) with a SPECS GmbH spectrometer (Model: XPS, Thermo K-Alpha).

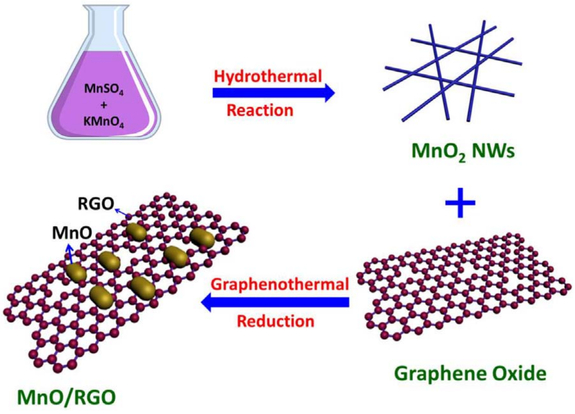

Fig. 1. Schematic representation of the preparation of MnO/RGO.

2.6. Electrode fabrication and electrochemical characterization

The electrochemical measurements were implemented with electrochemical work station (Model: CHI608C). The working electrode was synthesized with the active material, acetylene black and polyvinylidenefluoride at a ratio of 80:10:10, respectively. The above mixture was prepared as slurry by stirring overnight with the involvement of N-methyl-2-pyrrolidone as a solvent. The resultant slurry was layered on Cu foil as anode material for LIBs. The electrodes deal with the temperature of 80 °C for 12 h in the vacuum atmosphere. A series of electrochemical performances for LIBs were obtained by assembling CR2032 type coin cells in argon atmosphere glove box. The cell was employed with lithium foil as a counter and a reference electrode. A solution of 1 M $LiPF_6$ dissolved in EC/DMC as an electrolyte. The charge-discharge experiments were conducted in a voltage range of 0.05–3.0 V at various current densities.

3. Results and discussion

The fabrication process of the MnO/RGO composite is schematically illustrated in Fig. 1. Initially, 1D MnO_2 NWs were prepared by a hydrothermal method [27-29]. Fig. 2a shows FE-SEM image of MnO_2 NWs with smooth and uniform morphology. Here, we select the synthesized MnO_2 NWs with a length of several microns and a diameter of ~ 50 nm as a Mn source to prepare MnO/RGO. Interestingly, GO was reduced to RGO and MnO_2 NWs were converted into crystallized MnO NPs and anchored on RGO sheets during the graphenothermal process. Remarkably, the obtained composite was made up of nano-sized manganese oxide particles (Fig. 2b). The particle size of MnO is reduced to ~ 10 nm, which is obviously much smaller than MnO NPs prepared under similar conditions without GO (Fig. S1), which strongly suggest that RGO could promote the dispersion of MnO. The crystallinity and morphological features were further examined by TEM (Fig. 2d–f). Fig. 2d and e clearly show that the MnO particles were covered by semi-transparent graphene layers and the size of MnO particles (around 100 nm) were well matched with the SEM observation. The elemental information of the MnO/RGO composite is further studied by EDX (Fig. 2c), and Fig. S2 provides its elemental mapping, which presents the innate image of the distribution of Mn, C and O elements. Information regarding the edge of MnO nanoparticles was obtained with selected area electron diffraction (SAED) and indicates that the each MnO particles are highly crystalline (Fig. 2f).

Fig. 3a illustrates the XRD patterns of the MnO/RGO composite compared with MnO_2 NWs and GO. MnO/RGO composite exhibited lattice parameter of a = 4.445 Å with average crystallite size of 64 nm and all diffraction peaks corresponds to the cubic MnO (space group, $Fm\bar{3}m$, JCPDS card no. 75-1090) [30,31]. The diffraction peaks of MnO_2 are indexed to tetragonal MnO_2 (space group $I4/m$, JCPDS card